Available online at www.sciencedirect.com

SCIENCE DIRECT®

Journal of Catalysis 231 (2005) 201–212

JOURNAL OF CATALYSIS

www.elsevier.com/locate/jcat

The formation of isocyanic acid during the reaction of NH_3 with NO and excess CO over silica-supported platinum, palladium, and rhodium

Noel W. Cant [*], Dean C. Chambers, Irene O.Y. Liu

Department of Chemistry, Macquarie University, NSW 2109, Australia

Received 25 November 2004; revised 14 January 2005; accepted 18 January 2005

Abstract

The reaction between NH_3 and NO in excess CO over silica-supported platinum, palladium, and rhodium has been investigated for temperatures from 100 to 450 °C. As found previously for the corresponding reactions of H_2/NO/CO mixtures, isocyanic acid (HNCO) is produced with each catalyst. With Pd/SiO_2, the peak yield when NH_3 is used is 46% based on the total nitrogen converted and 55% based on the hydrogen taken from NH_3, with the remaining hydrogen converted to water. The reaction over Pt/SiO_2 requires a somewhat higher temperature and is more efficient with a maximum HNCO yield of 70% based on nitrogen and 95% on hydrogen. The near-absence of water as a product correlates with the high activity of platinum for the production of HNCO from H_2O/NO/CO mixtures, which in turn is driven by activity for the water–gas shift reaction. The peak yield of HNCO from NH_3/NO/CO mixtures is much lower with Rh/SiO_2 (10% based on nitrogen), and, unlike the yield of the platinum and the palladium catalysts, it is less than that observed during the $H_2 + NO + CO$ reaction (30%). In experiments using ^{15}NO and $^{14}NH_3$, the ^{15}N content of N_2, HNCO, and the end nitrogen of N_2O are similar, consistent with dissociation of both nitric oxide and ammonia to form a single surface pool of nitrogen atoms. However, neither dissociation is rapidly reversible, since there is little exchange of ^{14}N from ammonia into unreacted ^{15}NO, and significant formation of $^{15}NH_3$ is confined to Pt/SiO_2 at temperatures where it could be formed by hydrolysis of product $H^{15}NCO$. It is concluded that HNCO is formed by the rapid pick-up of surface hydrogen atoms by metal-bound NCO groups existing in equilibrium with N atoms and surrounding CO molecules. The trends in product distribution and in activity between the three metals can be rationalised in terms of competition between NO and CO for surface sites with CO favoured on Pt, NO favoured on Rh, and Pd exhibiting intermediate characteristics.

Keywords: NO reduction by NH_3 and CO; $NO + NH_3$; $NO + CO$; Isocyanic acid; HNCO; Pt/SiO_2; Rh/SiO_2; Pd/SiO_2; ^{15}N isotope

1. Introduction

In a rather remarkable series of four papers published in 1978, Voorhoeve and Trimble showed that cyanate compounds could be made in high yield by the reaction of H_2 and NO in a large excess of CO over unsupported platinum-group metal sponges [1–4]. When Pt and Rh were used, up to 98% of the NO in the feed could be converted to solid ammonium cyanate (NH_4OCN), which isomerised to urea when collected above 60 °C [1,3]. With Pd and Ir the major product was gaseous isocyanic acid (HNCO) [2,4]. Only one type of supported catalyst, Pt/Al_2O_3, was tested. No cyanates were seen in the products. Instead the major nitrogen-containing product was ammonia, which was attributed to the hydrolysis of NCO groups that form on platinum and then migrate to alumina [1]. Hecker and Bell subsequently reported that urea was produced during the reaction of H_2, NO, and CO mixtures over a reduced rhodium on silica catalyst [5]. They suspected, but were unable to prove, that isocyanic acid was formed when the catalyst was pre-oxidised but lost within their system, possibly as its non-volatile trimer, cyanuric acid.

In 1996 we used on-line FTIR analyses to show that gaseous isocyanic acid is a primary product of the reaction of H_2, NO, and CO over a Pt/SiO_2 catalyst [6,7]. The for-

---

[*] Corresponding author. Fax: 61 2 9850 8313.
E-mail address: noel.cant@mq.edu.au (N.W. Cant).

doi:10.1016/j.jcat.2005.01.022

mation of solid deposits was avoided altogether because the reactor, infrared cell, and all connecting tubing were maintained above 90 °C. The stoichiometry of HNCO formation appeared to be best described by the equation

$$NO + CO + 1.5H_2 \rightarrow HNCO + H_2O. \quad (1)$$

This could be rationalised in terms of existing knowledge concerning NO dissociation and the hydrogenation of metal-bound NCO groups. If Al_2O_3 was placed downstream of Pt/SiO_2, or if Pt/Al_2O_3 was used instead of Pt/SiO_2, then all HNCO was hydrolysed to ammonia and carbon dioxide:

$$HNCO + H_2O \rightarrow NH_3 + CO_2. \quad (2)$$

In subsequent work, we used an improved version of this system to examine HNCO formation from H_2, NO, CO mixtures over silica-supported Pt, Pd, and Rh [8,9]. Yields of HNCO were low with Rh/SiO_2, but Pd/SiO_2 was almost as effective as Pt/SiO_2. The data for the latter two catalysts also suggested that HNCO could be formed not only from hydrogen but also in a second stage in which ammonia, initially produced in parallel with HNCO by the $NO + H_2$ reaction, was itself converted to HNCO. In a recent publication we reported that HNCO can indeed be produced in this way from substoichiometric amounts of NH_3 in mixtures of NO and CO over both Pd/SiO_2 and Pt/SiO_2 catalysts [10]. It should be noted here that one of the papers of Voorhoeve and Trimble (and a patent) does include data showing that the addition of NH_3 to H_2, NO, CO or H_2O, NO, CO feeds increases the yield of ammonium cyanate over a platinum–10% rhodium sponge [4,11]. This was attributed to the scavenging of HNCO on the metal surface by ammonia, potentially allowing the production of 1 mole of NH_4OCN for each mole of NO reacted rather than the 0.5 mole of NH_4OCN possible if both nitrogen atoms in NH_4OCN must be supplied by NO. However, there was no suggestion that NH_3 could be converted to the NCO moiety itself, as indicated by our data for Pt/SiO_2 and Pd/SiO_2 [10].

The aim of the present work was to determine the characteristics of silica-supported Pt, Pd, and Rh for catalysis of the ternary mixture, NH_3 and NO in excess CO, in comparison with their characteristics for two binary reactions, $NO + NH_3$ and $NO + CO$. The third binary system, $NH_3 +$ CO, can be disregarded under steady-state conditions since thermodynamically possible yields, to either $HNCO + H_2$ or $HCN + H_2O$, are negligible at the temperatures of interest here. The present measurements have been carried out with NH_3 in stoichiometric excess over NO to preserve reducing conditions at all NO conversions, and they include comparison with the H_2, NO, CO system with the same concentrations. Isotope labelling is used to assess whether the nitrogen atoms derived from the NO or NH_3 are selectively converted to particular nitrogen-containing products.

The findings are of interest in the context of three-way catalysis as applied to motor vehicles, where NO, CO, and NH_3 can all be present in the converter under some conditions. The possible emission of isocyanic acid itself is not an issue in those systems, since further hydrolysis to ammonia by reaction (2) is certain to be fast on alumina and ceria–zirconia washcoats [8,9], especially given the high concentration of water present. Nonetheless, ammonia itself is undesirable since it plays a role in the production of haze-causing particulates in urban atmospheres [12].

2. Experimental

The test system and the analytical methods used in the present work were as described in detail previously [8,9]. In essence, catalyst samples (75 mg) were held in 4-mm i.d. Pyrex tubes with a test stream of 100 cm^3(STP)/min passing down flow. The feed was made by blending gas mixtures (supplied by BOC, Australia), with the use of electronic flow meters, to nominal concentrations of 3400 ppm CO, 1000 ppm NO, and, if present, 1500 ppm H_2 or 1000 ppm NH_3. The exit gas was analysed by a combination of gas chromatography (with a MTI Instruments model 200 instrument) and on-line FTIR (with a 16-cm path-length cell held at 90 °C) with spectra acquired every 10 min (3 min for the isotope experiments) with the use of a Nicolet Magna 550 instrument accumulating 64 scans at 0.25 cm^{-1} resolution. The HNCO concentrations were obtained by correcting the absorbance at 2284 cm^{-1} for a small contribution from CO_2 and then using a calibration factor obtained previously [8].

The concentrations of CO_2, CO, NO, N_2O, NH_3, and H_2O were obtained by processing various regions of the spectra with the program MALT developed by Griffith [13], which incorporates a least-squares fit against a set of synthetic spectra generated from the HITRAN data base [14]. In principle this method is absolute and does not require calibration. The accuracy for CO, CO_2, NO, and N_2O was ±5% at worst based on standard gas mixtures. Accurate standards were not available for NH_3 or H_2O, and the fitting procedure was less certain because of the sharpness of their lines. As noted later, mass balance calculations suggest that the concentrations determined for both NH_3 and H_2O are likely to be high by about 10%.

The ^{15}NO (Isotec Inc.; nominally 99.6% ^{15}N but with $\sim 4\%$ $^{14}N^{16}O$ and 3.3% $^{15}N^{18}O$ as impurities) was made up in 1% Ar in helium and interchanged back and forth with an equal concentration of ^{14}NO in helium alone with the use of a $1/16''$ 4-port valve (Valco Inc.). A quadrupole mass spectrometer with multiple ion monitoring (Balzers Thermostar model GSD 300T) was used to follow the disappearance of ^{14}NO (at $m/z = 30$) and the appearance of Ar ($m/z = 40$), ^{15}NO (31), and nitrous oxides containing one and two ^{15}N atoms (45 and 46). $^{14}N^{15}N$ and $^{15}N_2$ could also be obtained from the signals at 29 and 30 after careful correction of signals for the contributions arising through fragmentation of the various nitrous oxides. Analysis for $^{14}N_2$ and $^{14}N_2O$ was not possible because of the dominant contributions of CO and CO_2 to signals at 28 and 44, respectively. The concentrations of all four nitrous oxides, $^{14}N_2O$, $^{14}N^{15}NO$, $^{15}N^{14}NO$, and $^{15}N_2O$, could be obtained as part of the MALT fitting procedure for a region near 1200 cm^{-1}. The HITRAN database contains some line intensities for the ^{15}N-containing molecules attributable to earlier work by Toth [15–17]. The present work made use of a new set of unpublished line parameters, also determined by Toth, employed in a recent study of the isotopomers of nitrous oxide in the stratosphere [18]. Likewise, the concentration of ^{15}NO was obtained by incorporation of the intensities of its lines in HITRAN into the MALT fitting procedure. That of $^{15}NH_3$ was calculated from the intensity of a strong isolated line at 1174 cm^{-1} with the use of an extinction coefficient obtained from a reaction in which a known concentration of ^{15}NO was converted to $^{15}NH_3$ alone by reduction in a large excess of hydrogen over Pt/SiO_2.

Isotopic isocyanic acids were readily quantified from the FTIR spectra with the use of absorbances measured at 2284 cm^{-1} (predominantly due to $H^{14}NCO$) and 2270 cm^{-1} (where the contribution from $H^{15}NCO$ is at a maximum and that of $H^{14}NCO$ is approaching a minimum). Conversion factors were obtained at both wavenumbers for each species with the use of the calibration spectrum obtained previously for $H^{14}NCO$, under the assumption that the maximum extinction coefficient for $H^{15}NCO$ was the same as that of $H^{14}NCO$. These factors could then be applied to obtain the concentrations of the two isotopic acids from the spectra of mixtures by simultaneous solution. It may be noted here that changes in the concentrations of both isocyanic acids ($H^{14}NCO$ and $H^{15}NCO$) could also be observed through the intensities of the mass spectrometer signals at m/z of 42 and 43. However, the response was slowed because of buffering by traces of deposited material in an imperfectly heated section of the capillary leak to the mass spectrometer. The deposits did not affect other isotopic analyses with the mass spectrometer and could not influence the analyses by FTIR since that used separately heated lines.

The silica-supported catalysts used here were identical to those used previously. The Pt/SiO_2 and Pd/SiO_2 were from two series prepared and characterised by Burwell et al.; the platinum catalyst contained 1.1 wt% Pt with a dispersion of 40% [19], and the palladium catalyst 0.49 wt% Pd with a dispersion of 79% [20]. The base silica was a commercial silica gel (Davison grade 62, 285 m^2/g, particle size 180–210 µm). The Rh/SiO_2 was made in-house by impregnation of the same silica base with an aqueous solution of $RhCl_3$. It contained 0.50 wt% Rh with a dispersion of 38%, as determined by H_2 chemisorption after reduction. The catalysts were not subjected to further pre-treatment, beyond the final H_2 reduction at the end of preparation, before reaction. Rather, the catalysts were equilibrated in the reaction mixture itself by cycling the temperature up and then down over the range of interest until successive conversion-versus-temperature curves showed no change. The catalysts were found to stabilise (temperature for 50% conversion constant to ±3 °C) after two or three ramps and could be used for tens of runs thereafter without change in activity. Based on past work [21], this provides good assurance that the results for Rh/SiO_2 are not affected by residual chlorine. The curves shown in the figures that follow were obtained with the ramp rate set at 2 °C/min.

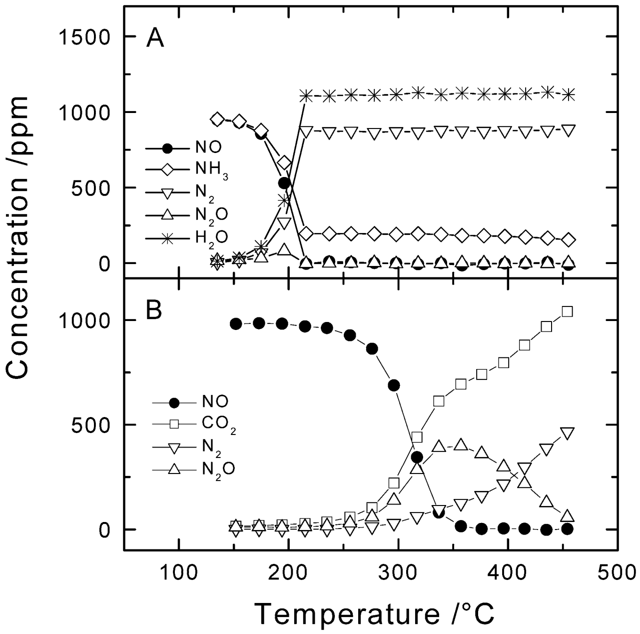

Fig. 1. Concentrations versus temperature during reactions of NO over 75 mg Pt/SiO_2 at a flow rate of 100 cm^3/min. A: between 1000 ppm NO and nominally 1000 ppm NH_3, B: between 1000 ppm NO and 3400 ppm CO.

3. Results

3.1. Reactions over Pt/SiO_2

Fig. 1 shows the temperature dependencies of the binary reactions of relevance here, $NO + NH_3$ and $NO + CO$, over 75 mg of the Pt/SiO_2. As in the subsequent figures, the concentration of CO has been omitted, since it was always in excess and at the concentration expected from the difference between the input value (3400 ppm) and that of the carbon-containing compounds in the output stream (CO, CO_2, and, in later figures, HNCO). As may be seen, the reaction of NO with NH_3 alone (Fig. 1A) is much faster than that with CO alone (Fig. 1B), with complete conversion of NO below 220 °C. The products are almost entirely N_2 and water with very little N_2O. Thus the reaction is predominantly

$$6NO + 4NH_3 \rightarrow 5N_2 + 6H_2O. \quad (3)$$

It may be observed that the concentration of water and the consumption of NH_3 are somewhat greater than implied by this stoichiometry. This is due to the fact that the FTIR method used for these species is uncalibrated and seems to overestimate the concentrations of both of these species by approximately 10%, as noted earlier.

The reaction between NO and CO (Fig. 1B) requires a temperature greater than 340 °C for complete conversion of

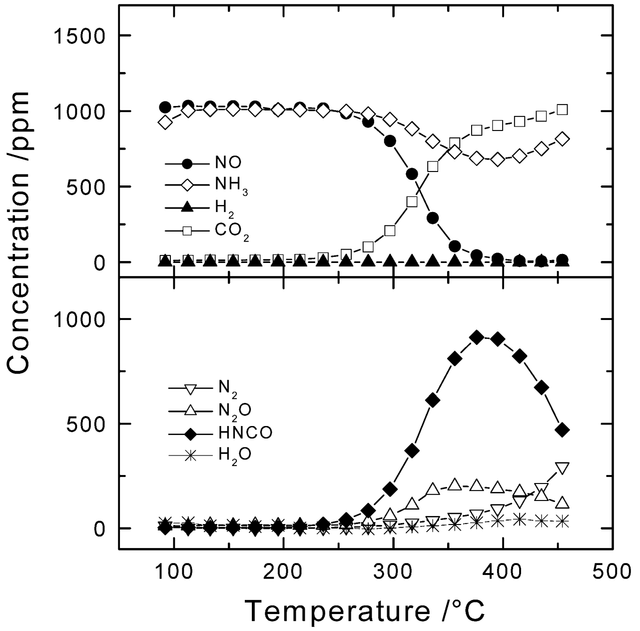

Fig. 2. Concentrations versus temperature for the reaction of a mixture of nominally 1000 ppm NH_3, 1000 ppm NO and 3400 ppm CO over 75 mg of Pt/SiO_2 with total flow rate of 100 cm^3/min.

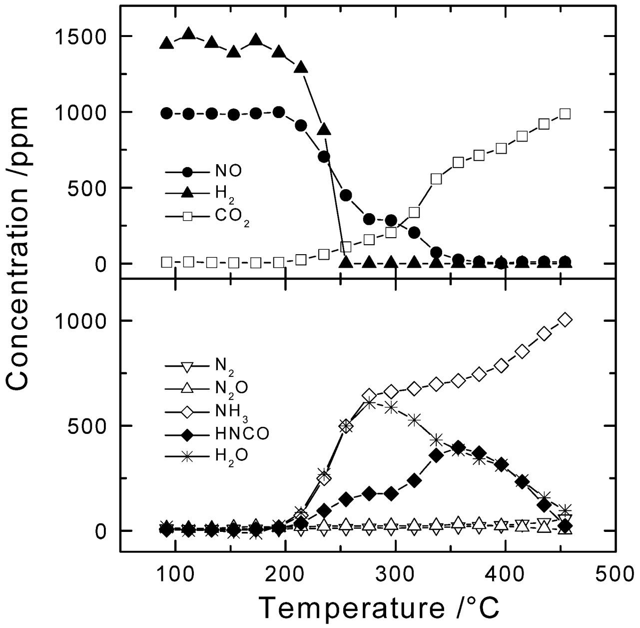

Fig. 3. Concentrations versus temperature for the reaction of a mixture of 1500 ppm H_2, 1000 ppm NO and 3400 ppm CO over 75 mg of Pt/SiO_2 with total flow rate of 100 cm^3/min.

NO. In accordance with the literature, N_2O and N_2 appear to form in parallel in the initial stages,

$$2NO + CO \rightarrow N_2O + CO_2, \qquad (4)$$

$$2NO + 2CO \rightarrow N_2 + CO_2, \qquad (5)$$

with (4) predominating at low temperature and (5) above ~ 400 °C, where there may be some contribution from the successive reaction of CO with N_2O.

The characteristics of the ternary reaction, $NH_3 + NO + CO$, over Pt/SiO_2 with the same input concentrations are illustrated in Fig. 2 (reactants and carbon dioxide in the upper panel and the remaining products in the lower). The temperature range over which the reaction proceeds is similar to that for the NO + CO reaction with suppression of the reaction of NO with NH_3, so that the NH_3 conversion is ~ 30% of that of NO up to 360 °C and less at higher temperatures. Isocyanic acid is the dominant nitrogen-containing product reaching 910 ppm at 376 °C, a yield of ~ 70% based on the sum of the nitrogen atoms in the NO and NH_3 converted. HNCO accounts for even more (~ 95%) of the H atoms in the NH_3 that does react. Thus very little water is formed. Instead the O atoms from the NO converted are very largely scavenged as CO_2. In approximate terms, the bulk of reaction can be represented as

$$2NO + NH_3 + 5CO \rightarrow 3HNCO + 2CO_2 \qquad (6)$$

with the remaining NO undergoing the standard reactions with CO, (4) and (5). In relative terms the concentrations of N_2O and N_2 show a dependence on temperature similar to that in Fig. 1B.

Fig. 3 shows the extent of formation of HNCO during a matching experiment between H_2, NO, and CO with the H_2 concentration set at 1500 ppm, so that the number of hydrogen atoms available for reaction is the same as in 1000 ppm NH_3. Conversion of NO commences at a much lower temperature than when NH_3 is used. All H_2 is consumed by ~ 255 °C with NH_3 and HNCO as the nitrogen-containing products, and the O atoms from NO are now converted to H_2O rather than CO_2. Thus over the temperature range where H_2 is consumed, the principal reactions appear to be

$$NO + 2.5H_2 \rightarrow NH_3 + H_2O \qquad (7)$$

and

$$NO + CO + 1.5H_2 \rightarrow HNCO + H_2O. \qquad (1)$$

However, although isocyanic acid formation plateaus at ~ 180 ppm between 260 and 300 °C, it increases again at higher temperature to a maximum of ~ 400 ppm at 360 °C, the additional hydrogen in HNCO being gained at the expense of water. Since CO_2 increases in parallel with HNCO, the overall stoichiometry for HNCO formation is trending towards

$$NO + 2CO + 0.5H_2 \rightarrow HNCO + CO_2. \qquad (8)$$

Finally, at higher temperatures still, HNCO production falls steadily until NH_3 eventually becomes almost the sole nitrogen-containing product, with a stoichiometry of

$$NO + CO + 1.5H_2 \rightarrow NH_3 + CO_2. \qquad (9)$$

The above equations involving three reactants, (1), (6), (8), and (9), should not be read as distinctly different reactions. Rather, they arise as the net result of shifting distributions in the concentrations and relative reaction rates of species on the Pt surface, coupled with a possible sequential reaction on the support, as discussed later.

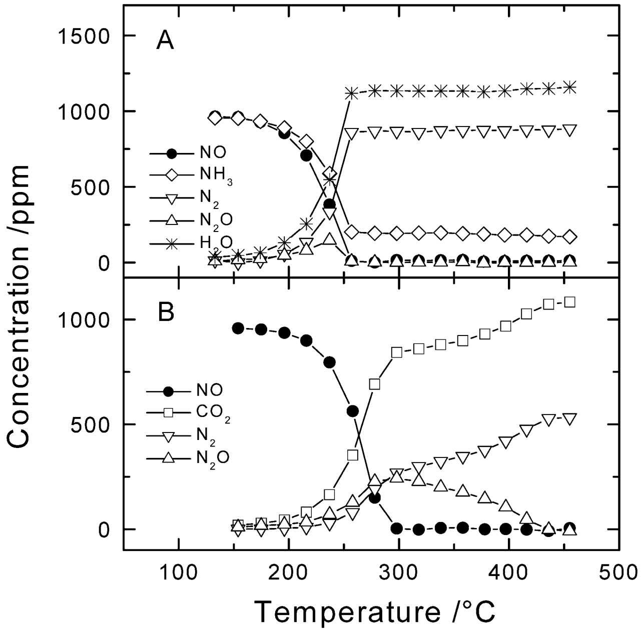

Fig. 4. Concentrations versus temperature during reactions of NO over 75 mg Pd/SiO_2 at a flow rate of 100 cm^3/min. A: between 1000 ppm NO and nominally 1000 ppm NH_3, B: between 1000 ppm NO and 3400 ppm CO.

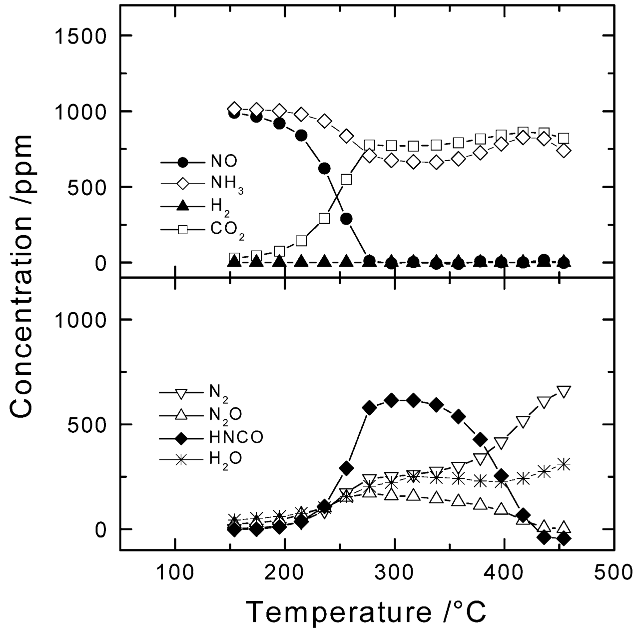

Fig. 5. Concentrations versus temperature for the reaction of a mixture of nominally 1000 ppm NH_3, 1000 ppm NO and 3400 ppm CO over 75 mg of Pd/SiO_2 with total flow rate of 100 cm^3/min.

Taken together, Figs. 2 and 3 show that NH_3 is a more effective source of hydrogen atoms for HNCO formation than is H_2, even when allowance is made for the greater number of N atoms converted when both NO and NH_3 are present (1270 ppm versus 1000 ppm when NO is used alone). In terms of selectivity, HNCO accounts for $\sim 70\%$ of the N atoms converted at the maximum when NH_3 is used but only $\sim 41\%$ when H_2 is used. The probable reasons for the difference are also discussed later.

3.2. Reactions over Pd/SiO_2

Fig. 4 shows the behaviour of the binary NO + NH_3 and NO + CO reactions over Pd/SiO_2. Reduction by NH_3 is somewhat faster, with 50% conversion of NO at 220 °C, whereas a temperature of 250 °C is required with CO. The product distributions are similar to those observed with Pt/SiO_2 (Fig. 1). Nitrogen is produced almost exclusively during reduction by NH_3, whereas the NO + CO reaction produces more N_2O than N_2 at low conversions with a gradual transition to mostly N_2 above 400 °C.

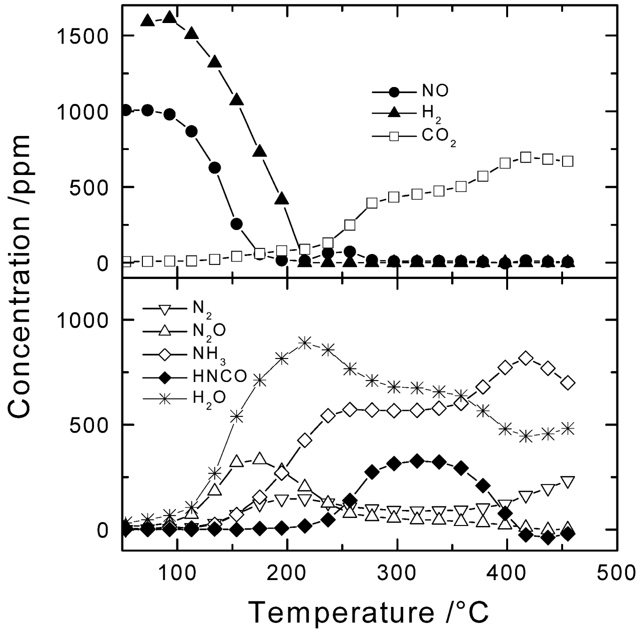

Fig. 6. Concentrations versus temperature for the reaction of a mixture of 1500 ppm H_2, 1000 ppm NO and 3400 ppm CO over 75 mg of Pd/SiO_2 with total flow rate of 100 cm^3/min.

The characteristics of the NH_3 + NO + CO reaction over Pd/SiO_2 are shown in Fig. 5. As is the case with Pt/SiO_2, removal of NO correlates with activity for the reaction between NO and CO while reduction by NH_3 is suppressed. Formation of HNCO occurs over a broad range of temperatures, with a maximum concentration of ~ 610 ppm near 320 °C. This corresponds to a HNCO yield of 46%, in terms of the nitrogen atoms converted, and 56% based on hydrogen removed from ammonia. The remaining hydrogen (i.e., 44%) forms water, which is quite unlike the situation with Pt/SiO_2, where production of water does not exceed 5% (Fig. 2).

The behaviour of Pd/SiO_2 for the corresponding reaction of NO with CO and 1500 ppm H_2 is illustrated in Fig. 6. The reaction is considerably faster than that with NH_3 (Fig. 5), and, unlike Pt/SiO_2 under the same conditions (Fig. 3), N_2O is the major nitrogen-containing product initially:

$$2NO + H_2 \rightarrow N_2O + H_2O. \qquad (10)$$

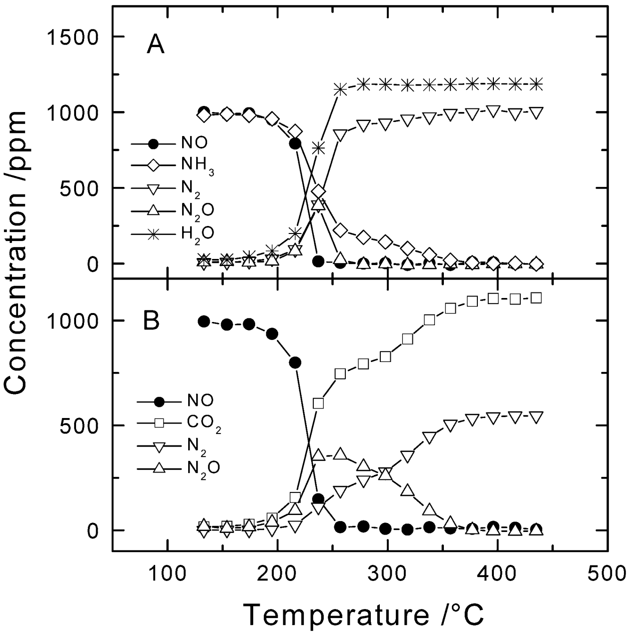

Fig. 7. Concentrations versus temperature during reactions of NO over 75 mg Rh/SiO_2 at a flow rate of 100 cm^3/min. A: between 1000 ppm NO and nominally 1000 ppm NH_3, B: between 1000 ppm NO and 3400 ppm CO.

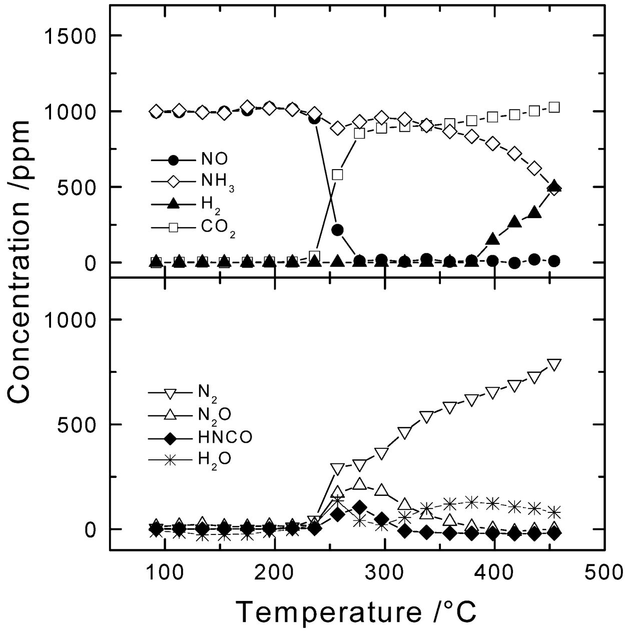

Fig. 8. Concentrations versus temperature for the reaction of a mixture of nominally 1000 ppm NH_3, 1000 ppm NO and 3400 ppm CO over 75 mg of Rh/SiO_2 with total flow rate of 100 cm^3/min.

Ammonia production takes over during the final stages of H_2 consumption (near 200 °C). At higher temperatures HNCO and CO_2 appear to form in parallel, as expected if some H_2 is converted according to reaction (8) or, more likely, if NH_3 forms in the initial part of the catalyst bed and then undergoes further reaction to HNCO according to reaction (6), as discussed later. HNCO formation exhibits a plateau of ∼ 320 ppm between 280 and 360 °C, above which there is a decline accompanied by increased formation of NH_3 and then N_2.

A comparison of Figs. 5 and 6 shows that NH_3 is a better source of hydrogen atoms for HNCO formation over Pd/SiO_2 than is H_2. This behaviour is the same as that of Pt/SiO_2.

3.3. *Reactions over Rh/SiO_2*

The temperature dependencies of the reactions of NO with NH_3, and with CO, over Rh/SiO_2 are shown in Fig. 7. Removal of NO occurs at very similar temperatures in the two systems, with 50% conversion at a temperature of 213 °C when NH_3 is used and at 214 °C when CO is used. As with the other two metals, the latter reaction favours N_2O as the product at lower temperature and N_2 at higher temperatures. Reduction by NH_3 gives rise to a slightly larger peak of N_2O at intermediate NO conversions than is evident with Pt/SiO_2 or Pd/SiO_2, but is otherwise similar. It may be noted from Fig. 7A that there is a continuous slow fall-off in the concentration of residual NH_3 at temperatures above that needed for complete consumption of NO. This is quite unlike the behaviour with Pt/SiO_2 and Pd/SiO_2 (Figs. 1A and 4A) and is probably due to NH_3 decomposition, since there is an accompanying slow rise in the N_2 concentration.

Fig. 8 shows the behaviour of Rh/SiO_2 as a catalyst for the reaction between NH_3, NO, and CO. The temperature range over which NO is consumed, 230–280 °C, is higher than for either of the binary reactions. The reaction that does occur is largely the NO + CO one, with only a small conversion of NH_3. The hydrogen atoms released from NH_3 are largely captured as water, with 90 ppm of NH_3 converted in this way at the small peak in H_2O production at 260 °C. Conversion to HNCO accounts for a maximum of 35 ppm NH_3 at 280 °C. The concentration of ammonia falls again above 380 °C, largely because of to direct decomposition, as shown by concurrent increases in the concentrations of N_2 and H_2. There may also be a small contribution from a reaction between N_2O and NH_3 that gives rise to the shallow peak in H_2O production near 380 °C.

The corresponding reaction of NO and CO in the presence of H_2 rather than NH_3 gives rise to a higher concentration of HNCO with a peak of ∼ 300 ppm at 240 °C (Fig. 9). Thus, unlike the situation with Pt/SiO_2 and Pd/SiO_2, H_2, not NH_3, is the better source of hydrogen atoms for HNCO formation from the ternary mixtures with the rhodium catalyst. The peak yield of HNCO is 10% with NH_3 but 30% with H_2, based on the nitrogen atoms converted. A major difference from the other metals is that hydrogen is never completely consumed during reaction over Rh/SiO_2. Indeed, after passing through a minimum of 350 ppm at 340 °C, the concentration of H_2 increases steeply again. This can be explained in terms of the decomposition of NH_3, which is the principal nitrogen-containing product at intermediate tem-

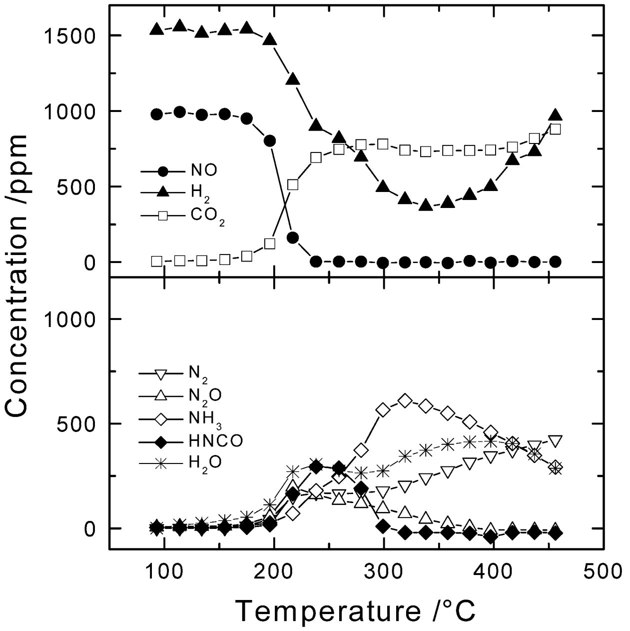

Fig. 9. Concentrations versus temperature for the reaction of a mixture of 1500 ppm H_2, 1000 ppm NO and 3400 ppm CO over 75 mg of Rh/SiO_2 with total flow rate of 100 cm^3/min.

peratures, but this decomposition declines in concert with the rise in H_2 concentrations above 340 °C.

3.4. Source of N atoms in the nitrogen-containing products

During the $NH_3 + NO + CO$ reaction, nitrogen-containing products may derive their nitrogen atoms from two sources. In principle, each product could draw a different fraction from each source, for example, HNCO from ammonia but N_2 and N_2O from nitric oxide. Isotope labelling experiments were carried out with ^{15}NO to determine whether a single pool of nitrogen, or distinguishable pools, are used. In each experiment the catalyst was allowed to stabilise in a flow of $^{14}NH_3$/^{14}NO/CO/He for an extended period, with the ^{14}NO/He stream then replaced by an equal flow of ^{15}NO/Ar/He containing the same concentration of ^{15}NO. Isotope concentrations were then followed until analyses were constant and the ^{15}NO was replaced by ^{14}NO again.

Fig. 10 shows the results for such an experiment carried out with Pd/SiO_2 after it had been allowed to stabilise for ∼ 25,000 s at 296 °C. The concentrations of $^{14}N^{15}N$, $^{15}N_2$, $^{15}N_2O$, and of the sum of the two mixed nitrous oxides (designated $^{14,15}N_2O$) all show step changes that are complete in a single mass spectrometer cycle of ∼ 20 s (Fig. 10A). There is no discernible delay relative to the corresponding signal of Ar, so the surface pool is too small to be measured. The concentrations derived from the FTIR measurements are more widely spaced (180 s apart), but the same step changes are apparent for the four nitrous oxides (Fig. 10B) and for the formation and subsequent disappearance of $H^{15}NCO$ and of $^{15}NH_3$ (Fig. 10C). Similar results were obtained in experiments at other temperatures, with lower concentrations of ammonia, and with Pt/SiO_2 in place of Pd/SiO_2.

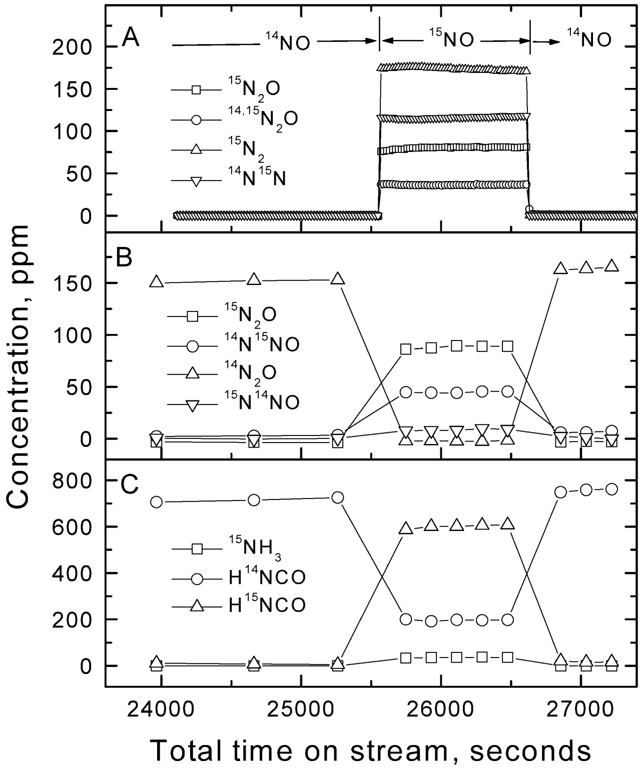

Fig. 10. Concentrations versus time during interchange of ^{14}NO and ^{15}NO for the reaction of 1000 ppm NO, 3400 ppm CO and nominally 1000 ppm NH_3 over Pd/SiO_2 at 296 °C. A: N_2 and N_2O measured by mass spectrometry, B: N_2O measured by FTIR, C: HNCO and NH_3 measured by FTIR.

If nitrogen atoms from ^{15}NO and $^{14}NH_3$ form a single surface pool, then each product should derive the same fraction of ^{15}N, f_{15}, from the pool. For HNCO and NH_3 this fraction is given by

$$f_{15} = {}^{15}N_i / \left({}^{14}N_i + {}^{15}N_i\right),$$

where $^{15}N_i$ and $^{14}N_i$ are the concentrations of the individual species. It is clear from the FTIR results that the nitrous oxide is almost entirely $^{14}N^{15}NO$ and $^{15}N^{15}NO$ when the feed is isotopically mixed and is hence derived by combination of intact ^{15}NO with surface ^{14}N or ^{15}N. The terminal nitrogen alone then represents the surface pool, in which case the appropriate formula for f_{15} based on the mass spectrometer analyses is simply

$$f_{15} = {}^{15}N_2O / \left({}^{14,15}N_2O + {}^{15}N_2O\right).$$

A limitation to the data for nitrogen is that direct analysis for $^{14}N_2$ was impossible because of the much higher concentration of CO. However, estimates based on the extent to which $^{14}N^{15}N$ and $^{15}N_2$, taken together, could account for the total amount of nitrogen determined by gas chromatography and for the fall in the intensity of the signal at $m/e = 28$ after substitution of ^{15}NO for ^{14}NO indicated that little $^{14}N_2$

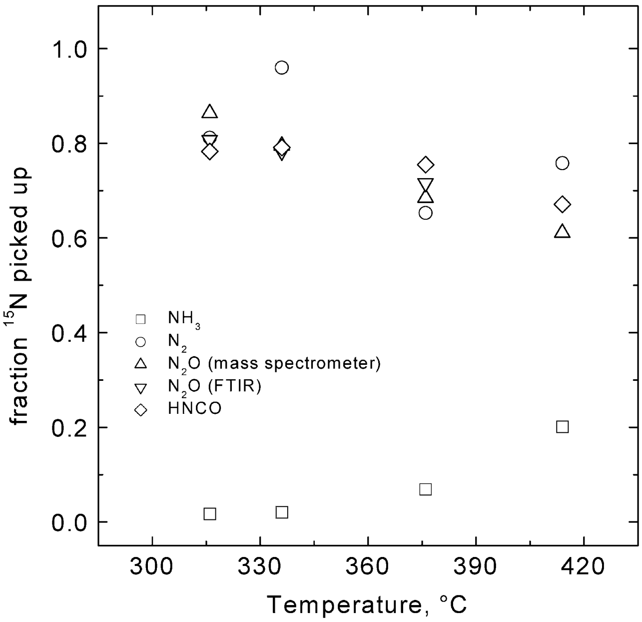

Fig. 11. Fraction ^{15}N versus temperature for the products of the reaction of 1000 ppm ^{15}NO with nominally 1000 ppm $^{14}NH_3$ and 3400 ppm CO over Pt/SiO_2.

was formed. In this case the fraction of ^{15}N can be calculated approximately as

$$f_{15} = 2\,^{15}N_2/\left(^{14}N^{15}N + 2\,^{15}N_2\right).$$

In addition to this approximation, the uncertainty in f_{15} for N_2 (∼ 15%) is several times that for the other species because of the corrections needed to account for fragmentation of the various nitrous oxides and for the ^{14}NO present as an impurity in the ^{15}NO used.

Data calculated from the set of isotope experiments carried out with Pt/SiO_2 at various temperatures are shown in Fig. 11. The ^{15}N contents of the surface pool from which HNCO and the end nitrogen of N_2O are derived are the same. The ^{15}N content of nitrogen is also the same to the limits of the approximation and uncertainty mentioned above. The small decline in ^{15}N content of these three products with increase in temperature is due to a diversion of ^{15}N to $^{15}NH_3$, which is small below 380 °C but increases to ∼ 20% at 416 °C. This increase is associated with the fall-off in HNCO production in Fig. 2. It reflects hydrolysis of $H^{15}NCO$ and/or hydrogenation of ^{15}N atoms derived from ^{15}NO, by surface hydrogen provided from $^{14}NH_3$. It should be noted here that FTIR analyses of unreacted nitric oxide when ^{15}NO was fed showed increases in the ^{14}NO content that were at most 4% for conversions where isotopic analysis was possible (NO conversions $< 90\%$, temperatures < 360 °C). Thus isotope exchange of ^{14}N atoms from ammonia into nitric oxide is negligible.

Fig. 12 shows the results of the isotope experiments with Pd/SiO_2. The pattern is the same as that found for Pt/SiO_2, with all products showing a similar value for f_{15}. There is little dependence on temperature and less $^{15}NH_3$ is formed, as expected on the basis that HNCO hydrolysis should be less at the lower reaction temperatures required with Pd/SiO_2. As with Pt/SiO_2, exchange of ^{14}N from ammonia into unreacted ^{15}NO was negligible for conversions where the concentration of residual nitric oxide remained sufficient for analysis (temperatures < 280 °C).

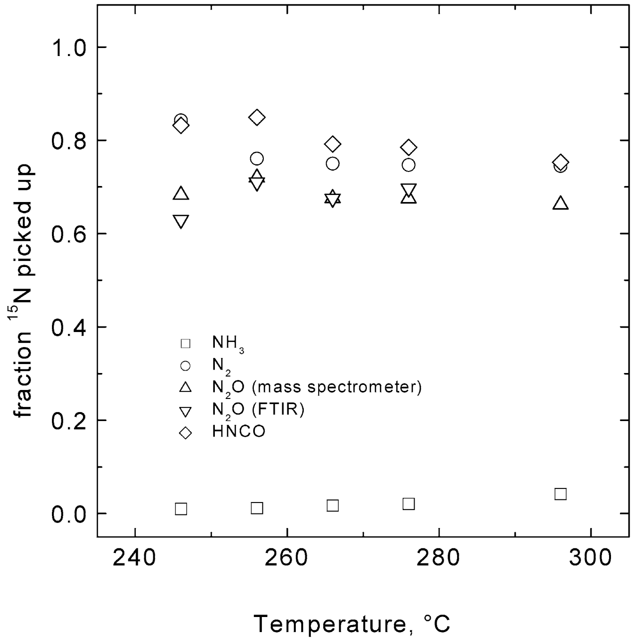

Fig. 12. Fraction ^{15}N versus temperature for the products of the reaction of 1000 ppm ^{15}NO with nominally 1000 ppm $^{14}NH_3$ and 3400 ppm CO over Pd/SiO_2.

Isotope experiments with Rh/SiO_2 were confined to two temperatures, 276 and 316 °C. The fraction of ^{15}N in the end nitrogen of nitrous oxide was indistinguishable from that in the nitrogen in both experiments, but the concentration of HNCO made was too small for isotopic analysis. The fractions of ^{15}N in ammonia were 9 and 15%, respectively, in line with the results for Pd/SiO_2 and Pt/SiO_2, given that intermediate temperatures were used.

4. Discussion

The present results show that isocyanic acid is readily made during the reaction of mixtures of NH_3, NO, and CO over silica-supported platinum group metals in a fashion similar to that reported previously for the H_2/NO/CO system [8,9]. Under the conditions used here, HNCO is the principal nitrogen-containing product over a wide range of temperatures with both Pt/SiO_2 and Pd/SiO_2, but only small amounts are formed with Rh/SiO_2. Ammonia is a more efficient source of HNCO than H_2 with both Pt and Pd, but the reverse is true with Rh/SiO_2.

The formation of HNCO and the other products of the ternary reactions can be rationalised with reference to the following species:

$$\begin{array}{l|l|l}
NO_{(g)} & {}^{*}NO \rightarrow {}^{*}N + {}^{*}O & N_{2(g)},\ N_2O_{(g)} \\
CO_{(g)} & {}^{*}N + {}^{*}CO \rightleftharpoons {}^{*}NCO & CO_{2(g)},\ HNCO_{(g)} \\
H_{2(g)} & {}^{*}H + {}^{*}H & H_2O_{(g)} \\
NH_{3(g)} & {}^{*}NH_3 \rightleftharpoons {}^{*}NH_2 + {}^{*}H & NH_{3(g)},\ N_{2(g)} \\
 & \quad \rightleftharpoons {}^{*}NH + 2H^{*} \rightleftharpoons {}^{*}N + 3H^{*} &
\end{array}$$

The left and right regions show reactants and products, respectively, and the centre section contains metal-bound entities (denoted by *) that can be formed by adsorption, dissociation, or combination. The differences in behaviour between the metals are interpretable in terms of the relative strengths of adsorption of CO and NO, with CO favoured on Pt, NO on Rh, and Pd showing intermediate characteristics [22].

First consider the situation for the Pt catalyst with only NO and CO present. Since CO displaces NO on Pt [23,24], and the reaction between them is strongly negative order in CO [25,26], the surface should be largely covered by CO in a steady state at low conversions. Reaction proceeds when CO desorption creates vacant sites that allow dissociation of the relatively few NO molecules present [27]. This deposits O adatoms that are rapidly removed as CO_2 by reaction with surrounding CO:

$$^{*}CO + {}^{*}O \rightarrow CO_{2(g)}. \tag{11}$$

Partner N adatoms can be removed through reaction with adsorbed NO to form N_2O,

$$^{*}N + {}^{*}NO \rightarrow N_2O_{(g)}, \tag{12}$$

which is favoured at lower temperature, or dimerisation to N_2,

$$^{*}N + {}^{*}N \rightarrow N_{2(g)}, \tag{13}$$

favoured at higher temperature. Both processes are hindered by nearly complete coverage by CO. The conjunction of N adatoms surrounded by CO molecules has the potential to form Pt-bound surface NCO groups, as indicated in the second row of the species diagram above. The population of Pt–NCO at reaction temperature must be small relative to CO since, although infrared studies show that such groups are stable at room temperature [28–30], they disappear at ∼ 50 °C [30], and only stable spectator Si–NCO groups on the support are seen during the NO + CO reaction with a dry feed [31]. However, this does not preclude the presence of a significant population of Pt–NCO groups relative to that of N adatoms under some conditions. Most authors believe that metal-bound NCO groups are not involved directly in the formation of either N_2O or N_2, although they have been included in some models for the reaction [32].

If ammonia (or hydrogen) is included in a NO/CO feed, then the formation of H adatoms by dissociation will provide additional paths by which N and O adatoms can be removed from the Pt surface. Comparison of Figs. 1A and 2 shows that CO strongly inhibits the reaction of NH_3 in the NH_3/NO/CO system, consistent with retention of a high CO coverage. When hydrogen atoms are released from NH_3 they end up almost exclusively (∼ 95%) in HNCO, whereas the oxygen atoms from NO are converted almost entirely to carbon dioxide rather than water. However, this strong tendency for hydrogen adatoms to generate HNCO rather than H_2O is not necessarily a result of direct competitive kinetics on the Pt surface, since water itself can react with NO and CO to form HNCO in high yield over the same temperature range [33] according to

$$H_2O + 2NO + 5CO \rightarrow 2HNCO + 3CO_2. \tag{14}$$

This reaction is facilitated by the activity of Pt for the water–gas shift reaction, $CO + H_2O$, which provides surface hydrogen and allows HNCO to form as long as NO is still available to deposit N adatoms and a high coverage of CO ensures the potential formation of Pt–NCO. The fall-off in HNCO above 400 °C in Fig. 2 is likely to be a consequence of a reduction in coverage by CO, which increases the surface population of N adatoms relative to NCO groups, thus favouring N_2 formation.

The $H_2 + NO + CO$ (Fig. 3) reaction is considerably faster than both the NO + CO (Fig. 1A) and $NH_3 + NO + CO$ (Fig. 2) reactions over Pt/SiO_2, with NO removal evident from 220 °C compared with 260 °C in those systems. Thus, unlike ammonia, H_2 must be able to dissociate on a surface that is largely covered by CO and facilitate reaction of NO, either by removal of O adatoms formed by direct dissociation of NO or through “hydrogen-assisted dissociation,” as discussed by Nieuwenhuys [22]. At temperatures below 300 °C the O atoms from NO are converted largely to H_2O (rather than the CO_2 seen during the $NH_3 + NO + CO$ reaction). In the same temperature range, the nitrogen atoms from NO react to form NH_3 rather than HNCO, which accounts for $< 10\%$ of the H_2 consumed below 300 °C. At higher temperatures the concentration of HNCO increases at the expense of H_2O. Clearly this can be interpreted as the redistribution of hydrogen from water to HNCO according to Eq. (14). Above 360 °C, both HNCO and H_2O decline, whereas NH_3 and CO_2 increase as expected if hydrolysis, reaction (2), is occurring. Silica has activity for that reaction at 315 °C and above [9].

The lower yields of HNCO when H_2 is used, compared with NH_3, are likely to be a consequence of a difference in the availability of hydrogen at the Pt surface. The full amount, 3000 ppm “H”, is deposited when 1500 ppm of H_2 is used, but a maximum of ∼ 800 ppm “H” is utilised from the 1000 ppm of NH_3. On mass action grounds, higher amounts of “H” will favour products with a high stoichiometric requirement for hydrogen, NH_3 and H_2O, which together require five “H” per NO (Eq. (7)). Correspondingly, restricting “H” will push the system towards HNCO, which requires only one “H” per NO by Eq. (8). This is true in practice. The same general principle applies if the H_2 concentration is reduced. In our previous work in which we used the same NO and CO concentrations as here, but with 400 ppm of H_2 rather than 1500 ppm, the peak yield of HNCO was considerably higher (> 600 ppm versus 400 ppm), whereas the concentrations of NH_3 and H_2O were below 100 ppm [10].

The above ideas can be readily modified to explain the behaviour of the other two metals. In contrast to the behaviour of platinum, gaseous NO will displace adsorbed CO from rhodium catalysts, whereas exposure of NO-covered Rh surfaces to CO leads to reaction and a rapid buildup of NCO species on the support [34]. The difference between the metals is also reflected in the kinetic orders for the NO + CO reaction, which are strongly negative in CO and positive in NO for Pt [25,26] but closer to zero in both reactants with Rh under most conditions [25,35–40]. Correspondingly, Rh surfaces tend to be populated by adsorbed NO molecules and N atoms under reaction conditions with relatively low concentrations of CO [22,39]. It is also apparent from Fig. 7 that Rh/SiO_2, unlike Pt/SiO_2, is not inherently more active for the $NO + NH_3$ reaction than the NO + CO reaction. These factors, a lower CO coverage and restricted access for NH_3 in particular, should mitigate against HNCO formation in the NH_3/NO/CO system over Rh/SiO_2, and the concentrations formed are indeed low (Fig. 8). If HNCO formation is highly restricted by the extent of NH_3 dissociation, then one might expect a greater yield in the H_2/NO/CO system, since H_2 should be dissociated more easily. This is also true (Fig. 9 versus Fig. 8). Indeed, the HNCO concentrations reached with H_2 are higher than in the corresponding reaction over Pt/SiO_2 (Fig. 3) for temperatures up to 300 °C. However, the second stage of reaction, which increases the HNCO yield above 300 °C with the Pt catalyst, is absent with Rh/SiO_2, because NO is completely removed in the first stage, so none remains to fuel the redistribution reaction, Eq. (14).

The activity of Pd/SiO_2 for the NO + CO reaction (Fig. 4B) is greater than that of Pt/SiO_2 (Fig. 1B), which is consistent with less inhibition of NO adsorption by CO [41]. It is thought that some N adatoms are present on Pd surfaces during the NO + CO reaction [42,43] and surface Pd–NCO species can be formed [44]. However, the $NO + NH_3$ reaction is slower over Pd/SiO_2 than Pt/SiO_2 (Fig. 4A versus 1A), which acts against HNCO formation in the NH_3/NO/CO system. A more significant reason why the maximum yield of HNCO is less with Pd/SiO_2 than Pt/SiO_2 (Fig. 5 versus 2) is that a considerable fraction of the hydrogen adatoms derived from ammonia are captured as water. As pointed out earlier, water is not a significant product in the NH_3/NO/CO system over Pt/SiO_2 because of the speed of the redistribution reaction (14). This process is facilitated by the high activity of platinum for the water–gas shift reaction and by the persistence of NO to temperatures above 340 °C (Fig. 2). With Pd/SiO_2, NO is completely consumed at a much lower temperature. The activity of Pd/SiO_2 for the water–gas shift reaction is also intrinsically less than that of Pt/SiO_2 [33,45]. Both factors act to minimise the possibility of redistribution of hydrogen from water to HNCO.

As with Pt/SiO_2, the $H_2 + NO + CO$ reaction over Pd/SiO_2 (Fig. 6) is much faster than either the NO + CO reaction (Fig. 4B) or the $NH_3 + NO + CO$ reaction (Fig. 5). However, the major product during the initial stages, N_2O, is different from the NH_3 produced by Pt/SiO_2. With the concentrations used here, 1000 ppm NO and 1500 ppm H_2, the formation of N_2O over Pd/SiO_2 means that NO can be fully consumed ahead of H_2 (at ~ 190 °C). When ammonia does become the major nitrogen-containing product immediately above 200 °C, it is H_2 that is fully consumed, and NO, at a low concentration, is observed again. HNCO is first observed at a similar temperature, and its concentration grows markedly at higher temperatures. Thus it seems quite possible that, in this regime, reaction is proceeding with rapid conversion of H_2 to NH_3 and H_2O at the front of the bed. This leaves some NO unreacted, and it can then participate in a secondary reaction with NH_3 and CO to produce HNCO on the remainder of the catalyst. It is noteworthy that formation of HNCO occurs over the same temperature range in the H_2/NO/CO system as the NH_3/NO/CO system with Pd/SiO_2 (Figs. 5 and 6).

The data for the isotope experiments illustrated in Figs. 10–12 for the $^{14}NH_3 + {}^{15}NO + CO$ reaction over Pt/SiO_2 and Pd/SiO_2 conform to the above picture. The simplest interpretation of these data is that the nitrogen-containing products are derived from a single pool of nitrogen adatoms formed from NH_3 and NO. This is as expected if ammonia dissociation is restricted by a high CO coverage, and surface hydrogen atoms, when they do form, are rapidly scavenged as HNCO, thus providing a strong driving force for the complete stripping of surface NH_x ($x = 1$–3) species. The near-absence of $^{15}NH_3$ at all temperatures with Pd/SiO_2, and below 370 °C with Pt/SiO_2, shows that the H adatom concentration is insufficient to allow conversion of ^{15}N adatoms, derived from ^{15}NO, to ammonia. The $^{15}NH_3$ concentration does increase when Pt/SiO_2 is used at higher temperatures, but this may be due to hydrolysis of $H^{15}NCO$. The present results cannot rule out some contribution from reactions in which NH_x species shed H while forming N_2 or N_2O (e.g., $^*NH + {}^*N \rightarrow N_2 + {}^*H$). However, they do preclude the formation of HNCO solely by combination of $^*CO$ and $^*NH_x$ ($x = 1$–3), since that could only yield $H^{14}NCO$.

The present isotopic results for nitrous oxide and nitrogen are similar to those of Hirano et al. [46] for the reaction of ^{15}NO with $^{14}NH_3$ alone on a Pt–Rh(100) single-crystal surface at similar temperatures and pressures. However, they are very different from those of Otto et al. [47] for the reaction of NO with NH_3 over Pt/Al_2O_3 at lower temperatures and with reactant pressures two orders of magnitude greater than here. According to their data, N_2O is formed largely from NO alone. This implies, in terms of reaction (12), that NO but not NH_3 is dissociated as far as N adatoms. (The actual mechanism suggested by Otto et al. [47] was that N_2O arose through the elimination of water from a surface complex formed by combination of two surface HNO groups.) In their experiments most nitrogen was formed with one N atom from NH_3 and one from NO. They suggested that surface NH_2 species combined with adsorbed NO to form a second complex that decomposed to form N_2 and H_2O. There is later experimental evidence that surface NH_2 groups are involved in the $NO + NH_3$ reaction on Pt(100) surfaces [48], and recent calculations indicate that NH_2 groups, and to an even greater extent NH groups, are stable with respect to N adatoms and H adatoms when the latter are both present on Pt crystal planes [49]. The probable reason for the absence of a predominant $^*NO + {}^*NH_2$ pathway in the experiments here is obvious. With carbon monoxide present, hydrogen adatoms are effectively scavenged by reaction with surface Pt–NCO groups to produce HNCO. This drives the rapid dissociation of NH_x species, restricting the extent to they can react with adsorbed NO, which is itself in short supply because CO coverages are high.

To our knowledge, there are no data in the literature on the relative activity of supported platinum-group metal catalysts of known area for the reactions investigated here. Table 1 provides a comparison for the four systems studied in terms of the temperatures required to give a turnover frequency of 0.01 molecules (NO) per surface metal atom per second. Data for the $NO + H_2$ reaction, taken from our previous work on the same catalysts under somewhat different conditions [9], are also included. The order of activity for the $NO + CO$ reaction (Rh > Pd > Pt) and for the $NO + H_2$ reaction (Pt > Pd ≫ Rh) matches that reported by Shinjoh et al. [50] for alumina-supported metals with unspecified metal areas. Kobylinski and Taylor [51] observed the same order under richer conditions, except that palladium was more active than platinum for the $NO + H_2$ reaction. The similarity between the three metals for the $NO + NH_3$ reaction is in accordance with the data of Bauerle et al. [52]. The data in Table 1 also emphasise the great inhibition attributable to CO in the two ternary reactions over Pt/SiO_2. The temperature required for the specified NO reaction rate is increased by ~ 120 °C relative to that needed for the $NO + NH_3$ reaction and ~ 180 °C relative to the $NO + H_2$ reaction. Inhibition by CO is nearly absent for Rh/SiO_2. The behaviour of Pd/SiO_2 is closer to that of Rh/SiO_2 than Pt/SiO_2, with CO causing limited inhibition (~ 50 °C) of the $NO + H_2$ reaction and having little effect on the $NO + NH_3$ reaction.

Table 1
Comparison of activities for reactions over Pt/SiO_2, Pd/SiO_2 and Rh/SiO_2

Reaction	Pt/SiO_2	Pd/SiO_2	Rh/SiO_2
$NO + CO$[a]	286 °C	251 °C	214 °C
$NO + NH_3$[a]	180 °C	221 °C	213 °C
$NO + H_2$[b]	46 °C	82 °C	196 °C
$NH_3 + NO + CO$[a]	300 °C	235 °C	240 °C
$H_2 + NO + CO$[a]	228 °C	133 °C	195 °C

[a] Temperatures giving a turnover frequency of 0.01 molecules (NO)/surface atom per second using 1000 ppm NO with CO, NH_3 and H_2 concentrations (when present) of 3400, 1000, and 1500 ppm, respectively.

[b] Temperatures giving a turnover frequency of 0.01 molecules (NO)/surface metal atom per second with NO = 2000 ppm and H_2 = 1000 ppm—see reference [9].

It may be noted from Table 1 that adding NH_3 to the NO/CO system lowers the rate of NO removal with Rh and Pt but increases it with Pd. There is no easy explanation for this behaviour in terms of simple competition. The acceleration with Pd implies that NH_3 gains access to the surface at the expense of some CO, so the rate of NO removal becomes intermediate between that of the $NO + CO$ reaction and the faster $NO + NH_3$ reaction. The retardation with Pt might be attributed to displacement of some NO by NH_3, on a largely CO-covered surface, thus lowering the NO coverage and reducing its dissociation rate. However, this does not seem reasonable as an explanation for the greater retardation seen with Rh, on which NO is expected to adsorb more strongly than CO. Displacement of CO by NH_3 would appear to be more reasonable. However, that should increase, not decrease, the NO removal rate since the $NO + NH_3$ reaction is faster than the $NO + CO$ reaction on Rh. A more complex behaviour must be present.

5. Conclusions

Isocyanic acid (HNCO) is formed by the reaction of NH_3 with NO in the presence of excess CO over silica-supported platinum, palladium, and rhodium in the same way that is possible with the use of H_2. The process is most efficient for Pt/SiO_2, with HNCO production exceeding 900 ppm when 1000 ppm of NO is totally converted. This is considerably more than is possible with H_2 for conditions where the number of hydrogen atoms available in the reductants is the same. Reaction over Pd/SiO_2 also produces substantial HNCO, again in higher concentration when NH_3 is used rather than H_2. However, the yields of isocyanic acid are much lower for reaction over Rh/SiO_2 with H_2, a more efficient source than NH_3. In each system, isocyanic acid appears to arise through the rapid capture of surface H atoms by metal-bound NCO groups forming from surface N atoms and adjacently adsorbed CO molecules. Isotope experiments using ^{15}NO and $^{14}NH_3$ on Pt/SiO_2 and Pd/SiO_2 indicate that nitrogen atoms, derived by dissociation of nitric oxide and ammonia, form a single pool on the metal surfaces, which randomly feeds through to isocyanic acid, nitrogen, and the end nitrogen of nitrous oxide. The initial dissociations are largely irreversible, since there is little isotopic exchange of ^{14}N from ammonia into unreacted ^{15}NO, or of ^{15}N from nitric oxide into ammonia. Some $^{15}NH_3$ does form during reaction over Pt/SiO_2 at temperatures above 370 °C, but this could arise through hydrolysis of $H^{15}NCO$. The differences between the three metals in terms of HNCO formation, and their relative activity for the various binary and ternary reactions, can be rationalised in terms of the relative adsorption strengths of CO and NO, with CO favoured on platinum and NO on rhodium, whereas palladium exhibits intermediate characteristics.

Acknowledgments

This work has been supported by grants from the Australian Research Council. The Pt/SiO_2 and Pd/SiO_2 catalysts used here were a past gift from Professor R. Burwell. We are grateful to Dr. R.A. Toth and Professor D. Griffith for provision of the database of line intensities for the ^{15}N isotopomers of nitrous oxide.

References

[1] R.J.H. Voorhoeve, L.E. Trimble, D.J. Freed, Science 200 (1978) 759.
[2] R.J.H. Voorhoeve, L.E. Trimble, Science 202 (1978) 525.
[3] R.J.H. Voorhoeve, L.E. Trimble, J. Catal. 53 (1978) 251.
[4] R.J.H. Voorhoeve, L.E. Trimble, J. Catal. 54 (1978) 269.
[5] W.C. Hecker, A.T. Bell, J. Catal. 88 (1984) 289.
[6] R. Dümpelmann, N.W. Cant, D.L. Trimm, Appl. Catal. B 6 (1995) L291.
[7] R. Dümpelmann, N.W. Cant, D.L. Trimm, J. Catal. 162 (1996) 96.
[8] N.W. Cant, D.C. Chambers, A.D. Cowan, I.O.Y. Liu, A. Satsuma, Top. Catal. 10 (2000) 13.
[9] D.C. Chambers, D.E. Angove, N.W. Cant, J. Catal. 204 (2001) 11.
[10] N.W. Cant, D.C. Chambers, I.O.Y. Liu, Catal. Today 93–95 (2004) 761.
[11] L.E. Trimble, R.J.H. Voorhoeve, United States Patent 4,174,377 (1979).
[12] M.P. Fraser, G.R. Cass, Environ. Sci. Technol. 32 (1998) 1053.
[13] D.W.T. Griffith, Appl. Spectrosc. 50 (1996) 59.
[14] L. Rothman, R. Gamache, R. Tipping, C. Rinsland, M. Smith, D. Benner, V. Malathy Devi, J.M. Flaud, C. Camy-Peyret, A. Perrin, A. Goldman, S. Massie, L. Brown, R. Toth, J. Quant. Spectrosc. Radiat. Transfer 48 (1992) 469.
[15] R.A. Toth, J. Opt. Soc. Am. B 3 (1986) 1263.
[16] R.A. Toth, J. Opt. Soc. Am. B 4 (1987) 357.
[17] R.A. Toth, Appl. Opt. 32 (1993) 7326.
[18] D.W.T. Griffith, G.C. Toon, B. Sen, J.-F. Blavier, R.A. Toth, Geophys. Res. Lett. 27 (2000) 2485.
[19] T. Uchijima, J.M. Herrmann, Y. Inoue, R.L. Burwell, J.B. Butt, J.B. Cohen, J. Catal. 50 (1977) 464.
[20] R. Pitchai, S.S. Wong, N. Takahashi, J.B. Butt, R.L. Burwell, J.B. Cohen, J. Catal. 94 (1985) 478.
[21] N.W. Cant, D.E. Angove, M.J. Patterson, Catal. Today 44 (1998) 93.
[22] B.E. Nieuwenhuys, Adv. Catal. 44 (2000) 259.
[23] R.M. Lambert, C.M. Comrie, Surf. Sci. 46 (1974) 61.
[24] M.F. Brown, R.D. Gonzalez, J. Catal. 44 (1976) 477.
[25] P. Granger, J.J. Lecomte, C. Dathy, L. Leclercq, G. Leclercq, J. Catal. 175 (1998) 194.
[26] D. Na-Ranong, T. Aida, H. Niiyama, Appl. Catal. A 234 (2002) 103.
[27] J.L. Freysz, J. Saussey, J.C. Lavalley, P. Bourges, J. Catal. 197 (2001) 131.
[28] F. Solymosi, T. Bansagi, J. Phys. Chem. 83 (1979) 552.
[29] R.J. Gorte, L.D. Schmidt, B.A. Sexton, J. Catal. 67 (1981) 387.
[30] J. Rasko, F. Solymosi, J. Catal. 71 (1981) 219.
[31] D.A. Lorimer, A.T. Bell, J. Catal. 59 (1979) 223.
[32] V.A. Matyshak, O.V. Krylov, Catal. Today 25 (1995) 1.
[33] N.W. Cant, D.C. Chambers, I.O.Y. Liu, Appl. Catal. B 46 (2003) 551.
[34] R. Dictor, J. Catal. 109 (1988) 89.
[35] W.C. Hecker, A.T. Bell, J. Catal. 84 (1983) 200.
[36] R.E. Hendershot, R.S. Hansen, J. Catal. 98 (1986) 150.
[37] C.H.F. Peden, D.W. Goodman, D.S. Blair, P.J. Berlowitz, G.B. Fisher, S.H. Oh, J. Phys. Chem. 92 (1988) 1563.
[38] H. Permana, K.Y.S. Ng, C.H.F. Peden, S.J. Schmieg, D.N. Belton, J. Phys. Chem. 99 (1995) 16344.
[39] H. Permana, K.Y.S. Ng, C.H.F. Peden, S.J. Schmieg, D.K. Lambert, D.N. Belton, J. Catal. 164 (1996) 194.
[40] J.H. Holles, M.A. Switzer, R.J. Davis, J. Catal. 190 (2000) 247.
[41] X. Xu, P. Chen, D.W. Goodman, J. Phys. Chem. 98 (1994) 9242.
[42] D.R. Rainer, S.M. Vesecky, M. Koranne, W.S. Oh, D.W. Goodman, J. Catal. 167 (1997) 234.
[43] D.R. Rainer, M. Koranne, S.M. Vesecky, D.W. Goodman, J. Phys. Chem. B 101 (1997) 10769.
[44] E. Ozensoy, C. Hess, D.W. Goodman, J. Am. Chem. Soc. 124 (2002) 8524.
[45] D.C. Grenoble, M.M. Estadt, D.F. Ollis, J. Catal. 67 (1981) 90.
[46] H. Hirano, T. Yamada, K.I. Tanaka, J. Siera, P. Cobden, B.E. Nieuwenhuys, Surf. Sci. 262 (1992) 97.
[47] K. Otto, M. Shelef, J.T. Kummer, J. Phys. Chem. 74 (1970) 2690.
[48] M.Y. Smirnov, D. Zemlyanov, J. Phys. Chem. B 104 (2000) 4661.
[49] A.R. Cholach, N.N. Bulgakov, B.E. Nieuwenhuys, Catal. Lett. 86 (2003) 9.
[50] H. Shinjoh, H. Muraki, Y. Fujitani, Stud. Surf. Sci. Catal. 30 (1987) 187.
[51] T.P. Kobylinski, B.W. Taylor, J. Catal. 33 (1974) 376.
[52] G.L. Bauerle, S.C. Wu, K. Nobe, Ind. Eng. Chem. Prod. Res. Dev. 14 (1975) 123.